

## 1 Introduction

As with any functional imaging, one of the critical factors in an investigator's ability to interpret Fluorescence Molecular Tomography (FMT) data is the reliability of the tomographic reconstructions. False negatives (missing signal) and false positives (artifacts) both hamper the accurate interpretation of data. Our study addresses the most prominent false positive artifacts with a reliable way of reducing their effect without a need for a priori assumptions about the concentration of fluorescence in the reconstruction.

## 2 Forward Model

FMT reconstructions use a forward model for light propagation through tissue based on the commonly used diffusion approximation. This approximation uses Green's functions to model the propagation of light between a grid of excitation light source locations, the voxels within the reconstruction, and the camera detectors. The resulting weight matrix has local maxima at the locations of the excitation light sources. This matrix times the distribution of fluorophore concentrations should yield the measured images, so a matrix inversion of the image data and the weight matrix produces the reconstructed distribution of concentrations. Because of the degeneracies in this inversion, fluorescence spread evenly over a range of depths can tend to get reconstructed at the locations of local maxima in the weight matrix, i.e. at the light source locations. Sources of fluorescence that are reconstructed at other locations in the volume are presumed to be more accurately placed. Multiple reconstructions of the same volume that use data obtained from illuminating the target at different sets of source locations would therefore have similar distributions of fluorescence except for the source-related artifacts. Our technique relies on this observation.

## 3 Matrix Inversion

The matrix inversion is an iterative process, so in the first few inversions,  $N$  reconstructions are computed, each using a subset of the grid of sources and their associated images. After these first few iterations, the reconstructions are combined, where each voxel in the combined reconstruction is the  $N$ th root of the product of the reconstructions at that voxel. Voxels with large values in only a subset of the reconstructions (source artifacts) are reduced in value, while voxels with consistent values across all reconstructions (real signal) retain their values.

The larger the value of  $N$ , the greater the reduction in intensity of the artifacts. However, the resolution of the resulting reconstruction degrades as the number of sources per reconstruction decreases, so the optimal value of  $N$  depends on the total number of sources for which data were acquired. Balancing these competing parameters is therefore critical. Fortunately, the set of sources in each reconstruction need not be unique, allowing larger values of  $N$  even with relatively small total numbers of sources. As long as each sub-reconstruction contains at least about 15 sources, the resolution of the resulting combined reconstruction will not suffer.

Optimizing the distribution of sources is also critical to the reconstruction quality. Ideally, the sources would be perfectly evenly distributed in each sub-reconstruction, i.e. each set of sources would have the same constant distance between a given source and its nearest neighbors. In practice with a rectilinear grid of sources, sometimes including extra sources outside a perfect rectangle or missing sources inside that ideal shape (e.g. Figure 1), we have to settle for a less than ideal distribution. Still, we can optimize the distribution of sources within that shape to maintain both the best possible average

distance between sources within a given sub-reconstruction and the same average distance between sources from one sub-reconstruction to the next. We do this using an approximate honeycomb pattern for each set of sources, as shown in Figure 1.

Because of the lower limit on the number of sources per sub-reconstruction described above, we would ideally always have 30 or more sources overall. For data where this is not the case, we can use  $N \geq 3$ , while ensuring that each source is missing from at least one sub-reconstruction and that each sub-reconstruction has at least 15 sources. This has the effect of reducing the source plane artifacts when the sub-reconstructions are combined without degrading the resolution of the final reconstruction.

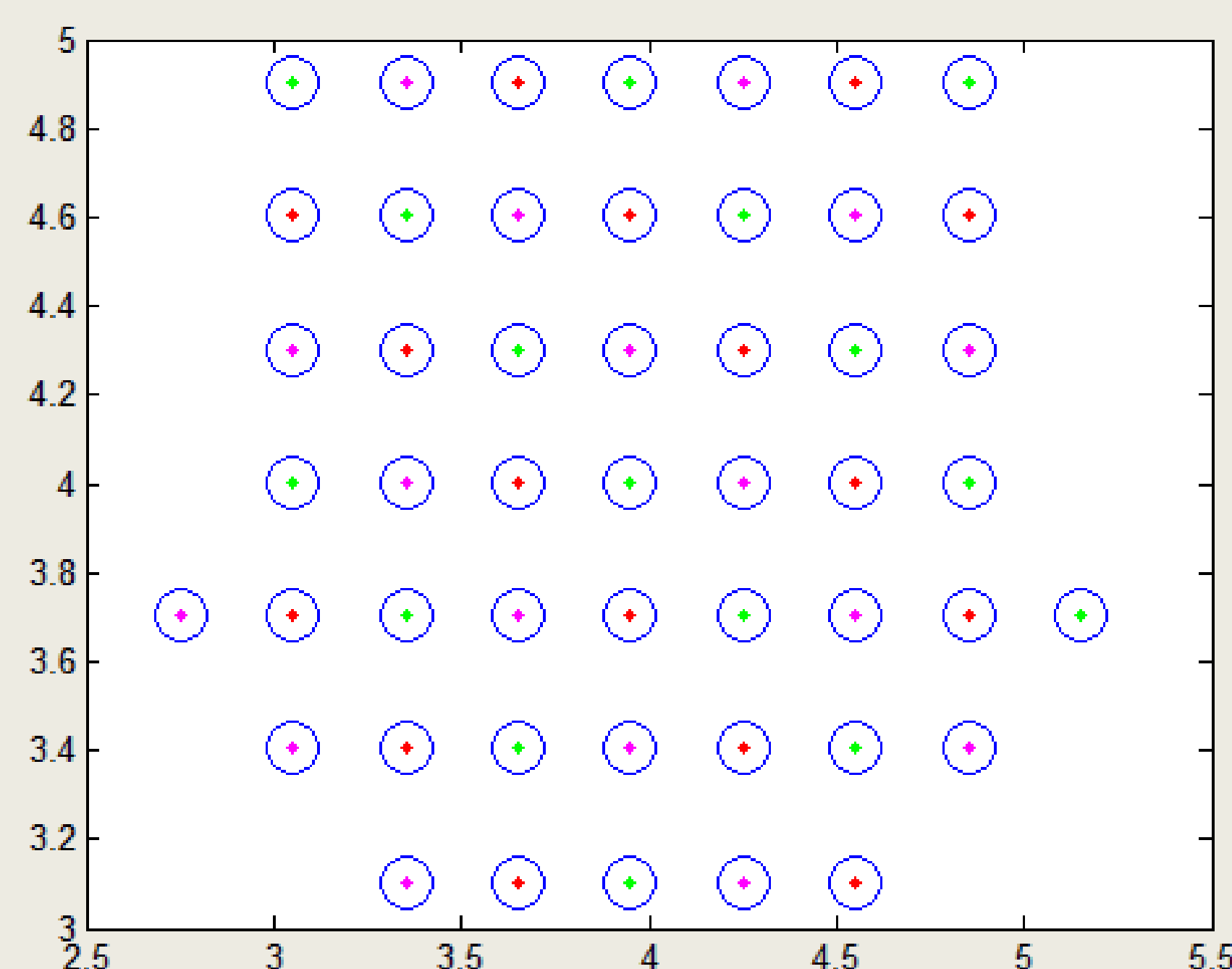


Fig. 1: The distribution of sources for the reconstruction shown in Figure 3B, with the Y axis inverted. Each sub-reconstruction has its set of sources in a given color, so this distribution represents  $N = 3$ . Distances on the axes are in cm.

## 4 Validation

This technique produces subtly different quantitative results compared to naive FMT reconstructions done without this correction. This is not surprising given that the fluorophores that are reconstructed at the source locations in the naive inversion represent *real* sources of fluorescence that have merely been allocated at the incorrect depth do to the combination of insufficient signal-to-noise and the local maxima of the weight matrix.

To validate the technique, we first imaged a series of solid resin phantoms, each with a 100  $\mu$ L inclusion of fluorescent dye at a different depth. These were reconstructed with the optimal number of separate reconstructions for the given scan field,  $N_{\text{split}} = 3$ . The linearity of recovered depth is excellent, consistent with the known depth of the inclusions as shown in Figure 2.

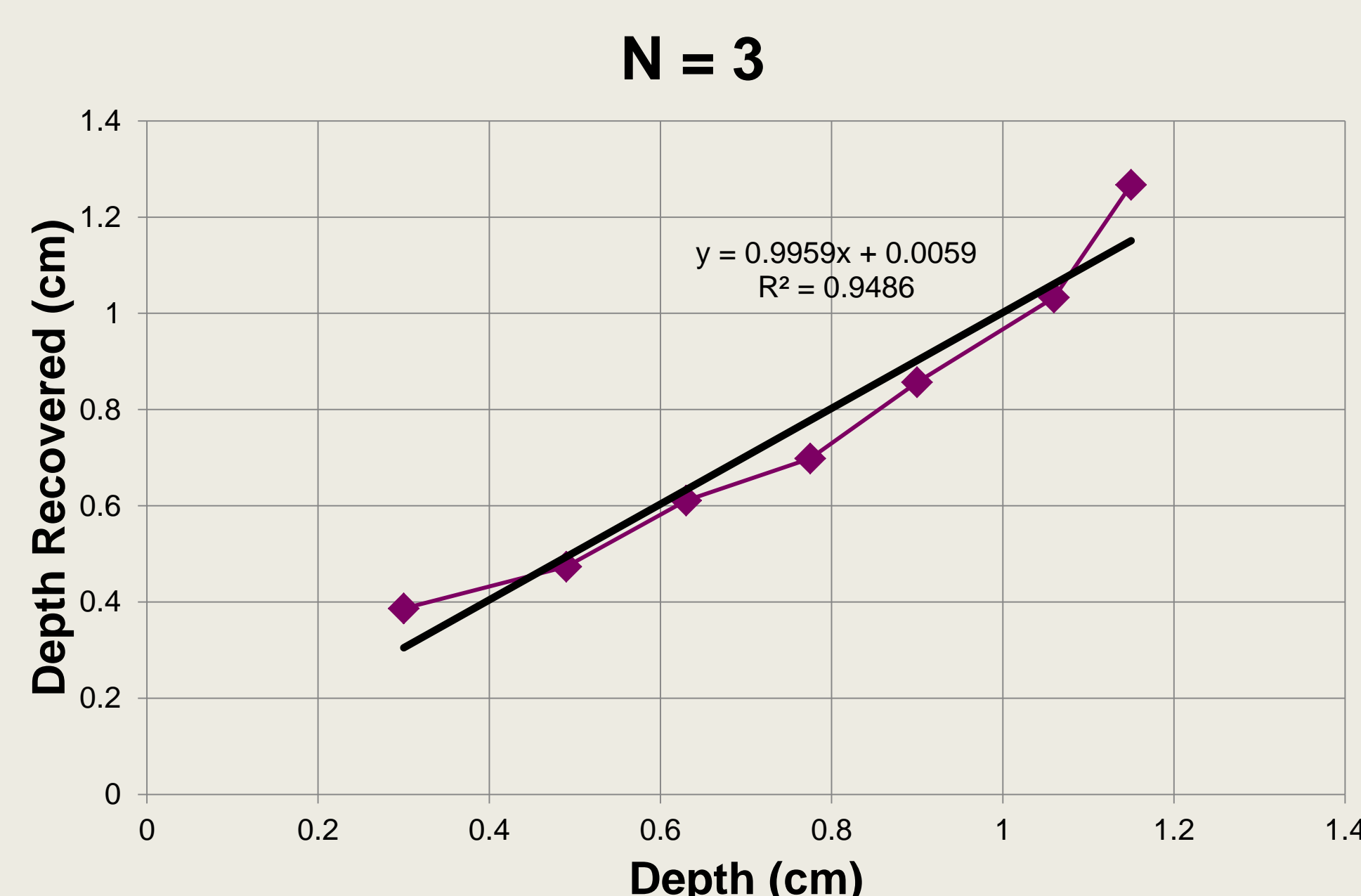


Fig. 2: Accuracy of depth recovery using phantoms with 100  $\mu$ L inclusions at a variety of depths. The best fit line is very close to the ideal 1:1.

We also performed a large number of reconstructions using *in vivo* data and compared the results with the naive reconstructions, i.e. those with  $N = 1$ . Some sample data are shown below. As described above, the source plane artifacts were dramatically reduced, while the recovered concentration varied somewhat compared to the naive reconstructions. In parts of the reconstruction above where the source plane artifacts were minimal or absent, the recovered concentrations changed very little when using  $N > 1$ , while areas directly above strong source plane artifacts increased in measured concentration compared to the naive reconstructions. Again, this is fully expected, since the artifacts represent real fluorescence that was allocated at the wrong depth. With the larger value of  $N$ , that fluorescence was allocated at the correct depth.

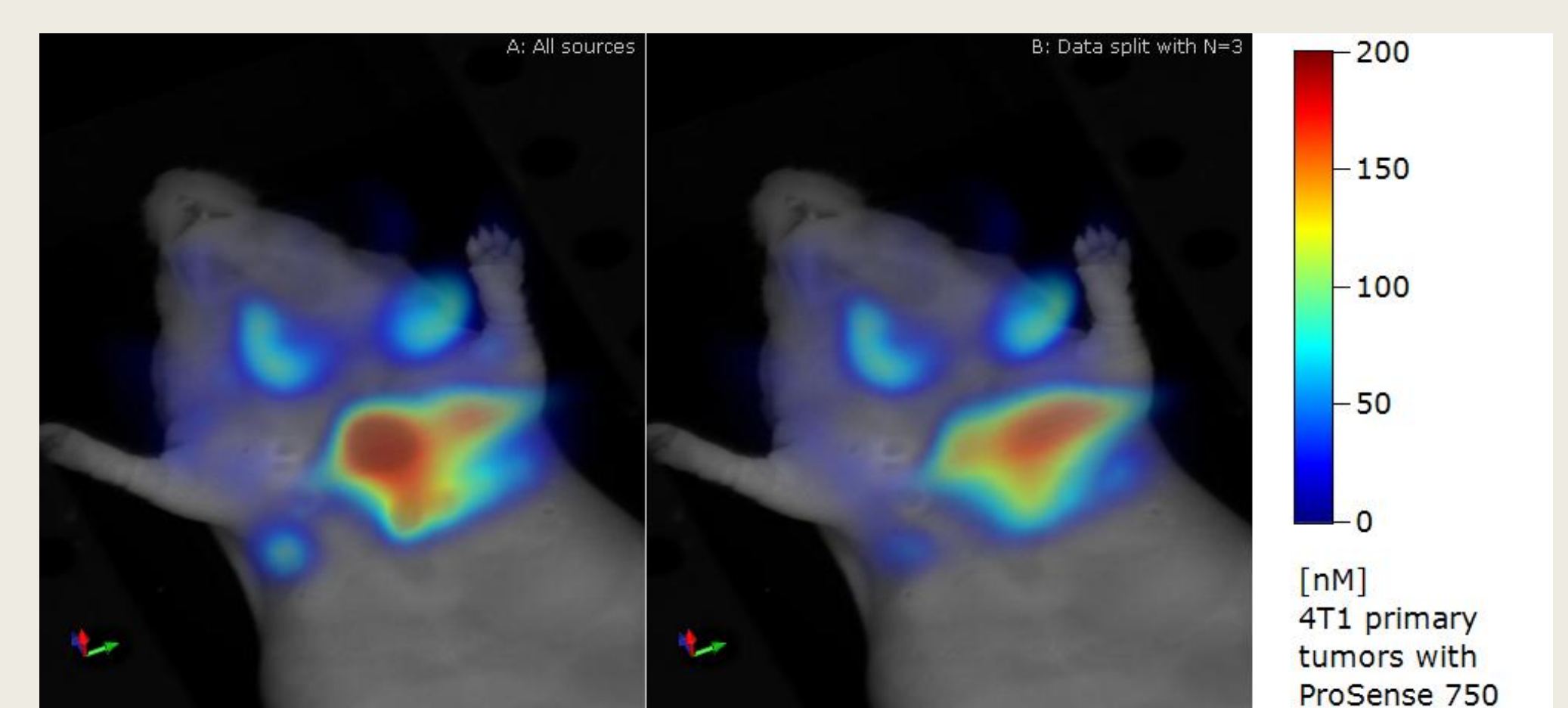


Fig. 3: 4T1 primary tumors in the upper mammary fat pads. The animal has been injected with ProSense™ 750, which metabolizes in the liver. Panel A shows the source artifacts in a naive  $N = 1$  reconstruction, especially below the liver, while Panel B, which uses the technique described in this poster with  $N = 3$ , reduces the intensity of the artifacts to an insignificant level.

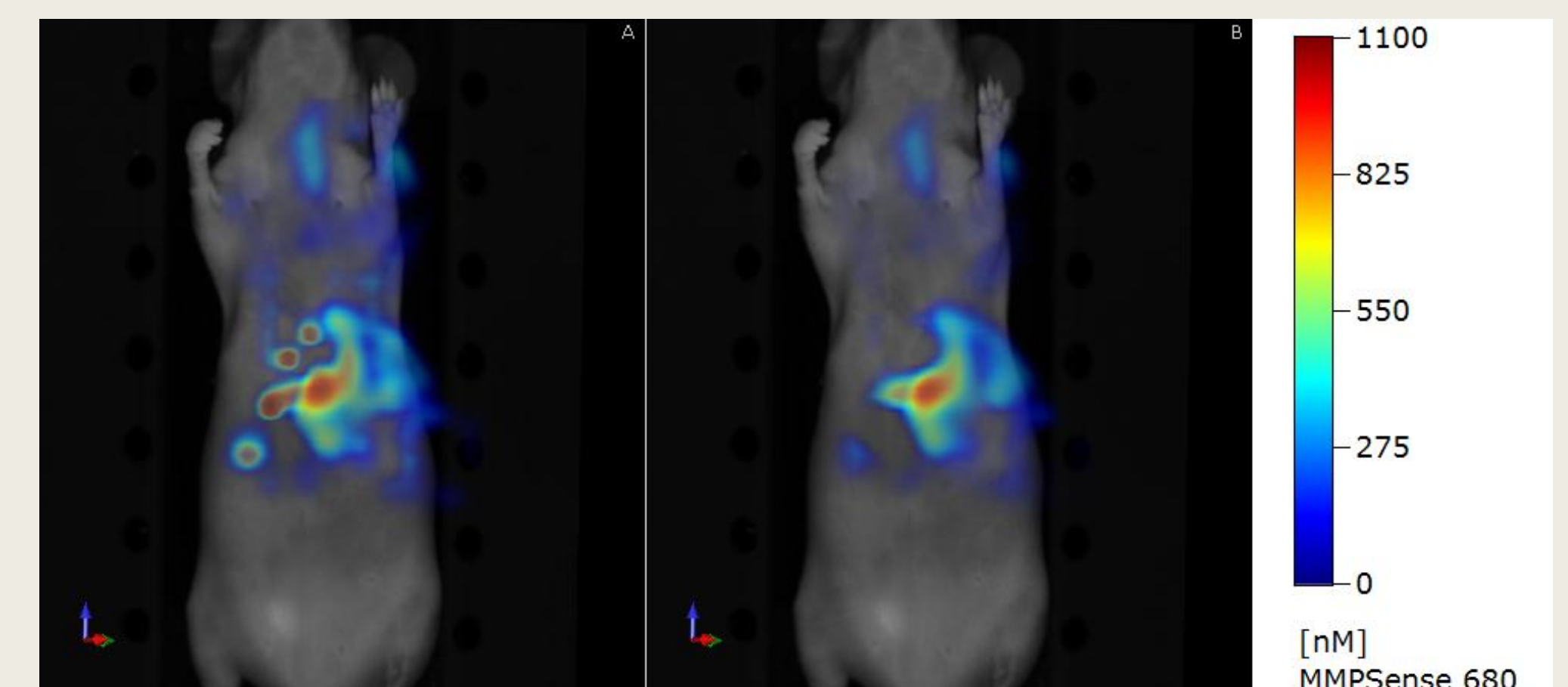


Fig. 4: An IP injection of MMPsense@ 680 in a healthy mouse. Panel A, which uses  $N = 1$  (the naive reconstruction) shows the source artifacts with an intensity greater than that of the true signal. In panel B, which uses the technique described in this poster with  $N = 3$ , the artifacts are eliminated or reduced to an insignificant level compared to the systemic agent.

## 6 Summary

We have demonstrated a novel approach to reconstruction of fluorescence signal in a turbid medium that reduces or eliminates the common false positive artifacts in locations where the Green's function has local peaks. The reconstruction is separated into two or more sub-reconstructions that are then combined multiplicatively. The result is that the artifact associated with a given source location only appears in one of the sub-reconstructions, and is subsequently reduced during combination with the other sub-reconstructions. This technique has no negative effect on depth recovery, and produces quantitative results that are consistent with naive reconstruction methods that include source plane artifacts at some locations.